Cell Reports, Volume *36*

Supplemental information

Paradoxical hyperexcitability from $Na_V1.2$ sodium channel loss in neocortical pyramidal cells

Perry W.E. Spratt, Ryan P.D. Alexander, Roy Ben-Shalom, Atehsa Sahagun, Henry Kyoung, Caroline M. Keeshen, Stephan J. Sanders, and Kevin J. Bender

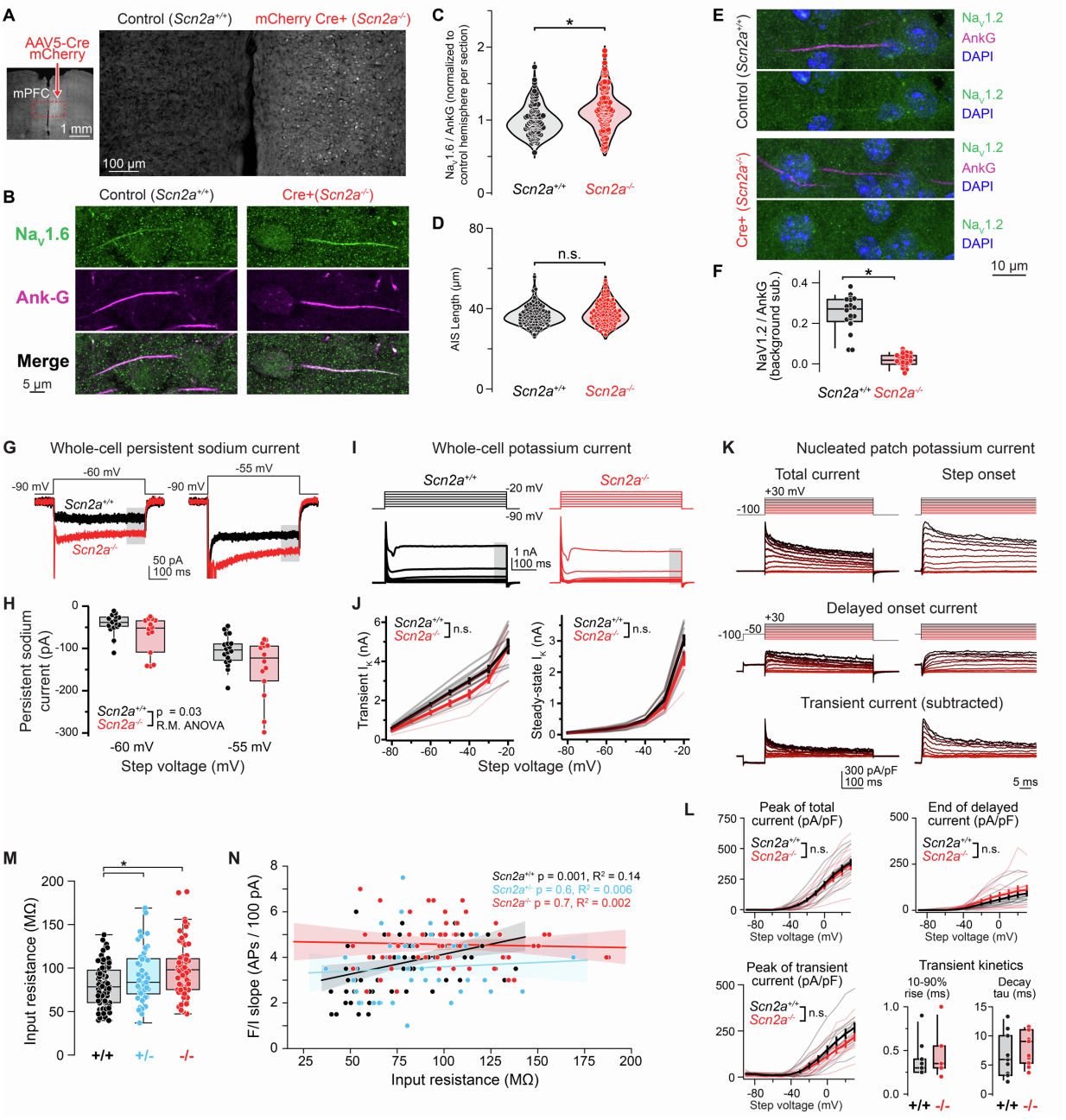

Figure S1, related to Fig. 1: Currents and intrinsic properties of *Scn2a*$^{-/-}$ cells

A: Example injection of unilateral AAV5-mCherry-Cre into mPFC of mouse at P28. Comparisons were made between injected (*Scn2a*$^{-/-}$) and control (*Scn2a*$^{+/+}$) hemispheres. Scale bars are 1 mm and 100 µm.

B: Immunostaining of $Na_V1.6$ and ankyrin-G in layer 5 of both hemispheres. Scale:5 µm.

C: Quantification of $Na_V1.6$ staining. Intensity in each AIS was normalized to ankyrin-G. Data were then normalized to mean ankyrin-G intensity of all initial segments analyzed within each section (both hemispheres). Data plotted as violin plots with individual initial segments as single points. *: $p < 0.001$, Mann-Whitney. n = 126 WT and 123 *Scn2a*$^{-/-}$ initial segments across 3 animals.

D: AIS length was not altered by $Na_V1.2$ knockout ($p = 0.14$, Mann-Whitney).

E: Immunostaining of $Na_V1.2$ and ankyrin-G in both hemispheres. Scale: 10 μm.

F: Quantification of $Na_V1.2$ staining. n = 20 WT, 24 *Scn2a*$^{-/-}$; *: $p < 0.0001$, Mann-Whitney. $Na_V1.2$ intensity is not different than 0 ($p = 0.07$, one sample t-test). Box plots in F, H, M, L are medians and quartiles with 90% tails.

G: Example persistent sodium currents from *Scn2a*$^{+/+}$ (black) and *Scn2a*$^{-/-}$ (red) cells for voltage steps from -90 to -60 or -55 mV.

H: Summary of persistent currents for each voltage step. $p = 0.03$, repeated measures ANOVA across genotypes. n = 18 WT, 14 *Scn2a*$^{-/-}$ cells.

I: Example whole-cell potassium currents from *Scn2a*$^{+/+}$ (black) and *Scn2a*$^{-/-}$ (red) cells for voltage steps from -90 to -20 mV in 10 mV increments.

J: Summary for transient onset current and steady state current (last 50 ms before voltage step offset, grey area in I). Thick lines and bars are mean ± SEM across population. Light, thin lines are data from single cells (n = 11 WT, 10 *Scn2a*$^{-/-}$ cells). Data analyzed with repeated measures ANOVA.

K: Example nucleated patch potassium currents for voltage steps from -100 to +30 mV (color coded from red to black for increasing step amplitude). Total current for 500 ms step and highlight of step onset are shown. Delayed onset currents measured following 100 ms prepulse to -50 mV; transient currents were calculated by subtracting delayed onset current from total current. All currents normalized to patch capacitance.

L: Summary for peak of total current (at onset), the last 50 ms of the delayed current, the peak of the transient current (onset), and the kinetics of the transient current. Amplitudes shown and analyzed as in J; Kinetics analyzed with Mann-Whitney statistics. n = 11 WT, 11 *Scn2a*$^{-/-}$ cells.

M: Input resistance for all cells in Fig. 1. *: $p < 0.001$, Kruskall-Wallis test, Wilcoxon rank sum posthoc test. n = 77 WT, 40 *Scn2a*$^{+/-}$, 60 *Scn2a*$^{-/-}$ cells.

N: Input resistance vs. the slope of the F/I curve between 100 and 300 pA for each cell. Data color-coded as in K. Lines and shaded regions represent best linear fit and 95% confidence intervals. p and R2 values noted in figure. n = 77 WT, 40 *Scn2a*$^{+/-}$, 60 *Scn2a*$^{-/-}$ cells.

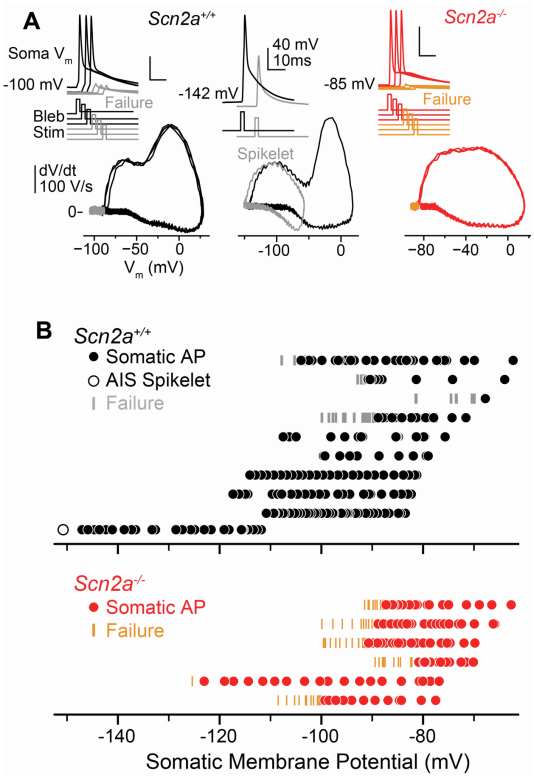

Figure S2, related to Fig. 2: Somatic invasion of APs initiated from axonal bleb

A: Examples of successive single APs evoked with 2 ms, 2 nA current injection at bleb. Somatic V_m was hyperpolarized on successive trials with steps of somatic bias current, eventually hyperpolarizing to the point that no APs could be evoked via bleb current injection. Bleb stim timing offset for clarity. Similar effects noted in WT and *Scn2a*$^{-/-}$ cells. Spikelet observed once at -150 mV in WT cell (middle). Note differences in X scale for each phase-plane.

B: Summary across all WT and *Scn2a*$^{-/-}$ cells. Each row is a single cell, with somatic AP successes, failures, and spikelets at each somatic voltage plotted as closed circles, vertical lines, and open circles, respectively. n = 10 WT and 6 *Scn2a*$^{-/-}$ cells.

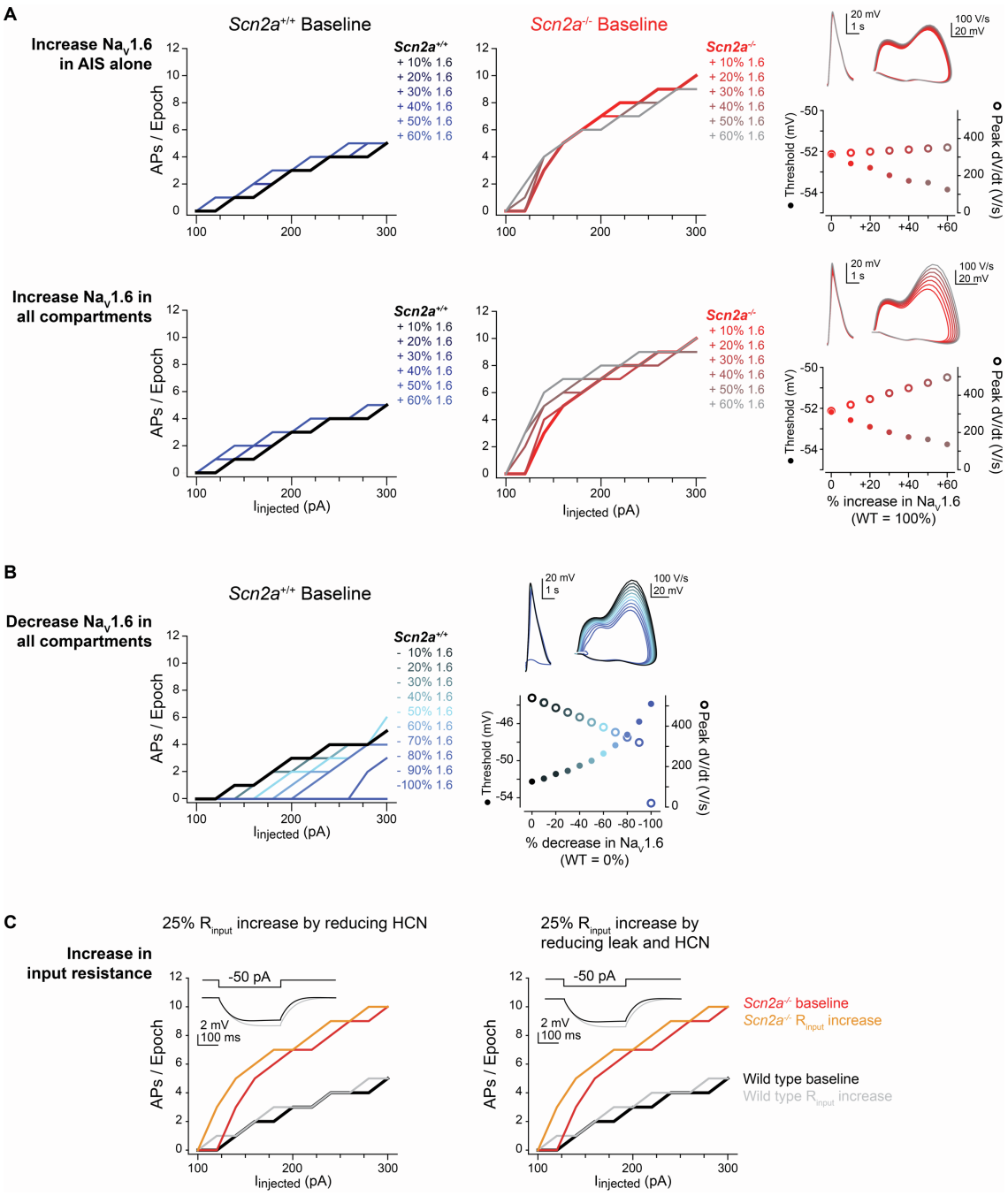

Figure S3, related to Fig. 3: Altering $Na_V1.6$ density or increasing input resistance in models do not recapitulate empirical results.

A: Increased $Na_V1.6$ density (10% increments over baseline levels in each compartment) either in the AIS alone (top row, matching immunofluorescence and persistent current observations) or in all compartments (bottom row, assuming similar effects as those observed in AIS) has minimal effect on F/I curves in WT models (left, blue), or in *Scn2a*$^{-/-}$ models (right, red). Note that, in both cases, AP threshold hyperpolarizes with increased $Na_V1.6$ density, an effect not observed *ex vivo* (Fig. 1).

B: Decreased $Na_V1.6$ density (10% increments from baseline WT levels to full knockout, all compartments) increases AP threshold and reduces F/I curve. Contrast with $Na_V1.2$ knockout (Fig. 3).

C: Increases in input resistance, mimicking ~25% increases observed in empirical data (Fig. S1), were modeled by reducing HCN channel density alone (left), as these channels are principal contributors to input resistance in thick tufted pyramidal cells (Dembrow et al., 2010), or by reducing leak current to zero and additionally reducing HCN channel density (right, as elimination of leak currents alone cannot increase input resistance by 25%). Different input resistance configurations were modeled in wild type and *Scn2a*$^{-/-}$ cells. Note that increased input resistance shifts the onset of the F/I curve left, an effect not observed in empirical data. Furthermore, increasing input resistance alone does not evoke marked increases in excitability.

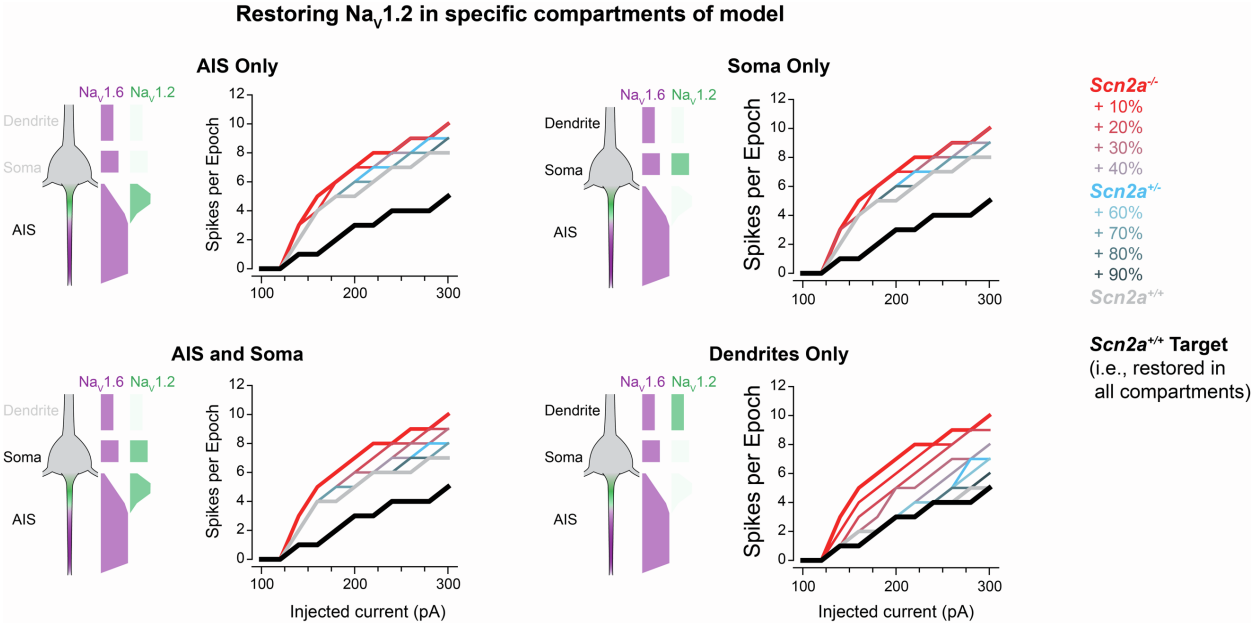

Figure S4, related to Fig. 4: Limitations in space-clamp of injected conductances prevents full restoration of *Scn2a*$^{+/+}$-like F/I curves in *Scn2a*$^{-/-}$ cells.

Compartmental models in which Na$_V$1.2 density was progressively restored from *Scn2a*$^{-/-}$ to *Scn2a*$^{+/+}$ levels (10% increments) in specific compartments. Data compared to "target" of complete restoration in all compartments (black: AIS, soma, dendrite). Note difficulty separating *Scn2a*$^{-/-}$ curve from 80% restoration curve in AIS or soma-only conditions.